



Observational study on air-water interactions over Poyang lake during a cold season

XIMING LIU, HONGBIN CHEN*, YANAN LIU**, LUJUN JIANG** and HONGYAN CHEN*

Ximing Liu, Jiangxi Institute of Meteorological Science, Nanchang, 330096, Nanchang, China

**Hongbin Chen, Chinese Academy of Sciences, China, Beijing, 100864, Beijing, China*

***Yanan Liu, Jiangxi Institute of Meteorological Science, Nanchang, 330096, Nanchang, China*

(Received 18 July 2022, Accepted 8 April 2024)

e-mail : changelyn2022@163.com

सार – एक झील में क्षेत्रीय मौसम और जलवायु के सबसे बुनियादी घटक हैं - ऊष्मा व ऊर्जा बजट और वाष्पीकरण जोड़ील और वायुमंडल के बीच परस्पर क्रियाओं से नियंत्रित होते हैं। पोयांग झील चीन की सबसे बड़ी मीठे पानी की झील है। दक्षिणपूर्वी चीन में यांगत्ज़ी नदी के मध्य और निम्न जलग्रहण क्षेत्र में स्थित इस उथली झील का सतह क्षेत्र वर्ष भर वर्षा के आधार पर बदलता रहता है। 1 दिसंबर 2020 से 28 फरवरी 2021 तक शीत ऋतु के दौरान सतह ऊर्जा प्रवाह और अन्य संबंधित वायुमंडलीय/जलीयचरों को मापने के लिए झील के उत्तर-पूर्व में खुले पानी वाले क्षेत्र में एक स्टील प्लेटफॉर्म बनाया गया। नतीजे बताते हैं कि जलीय सतह का औसत तापमान 2 मीटर ऊंचाई के वायु तापमान से 1.25 डिग्री सेल्सियस अधिक था, हालांकि तापमान में कभी-कभी थोड़े समय के लिए बदलाव होता है। औसत पवनगति और घर्षण वेग कम था, जिससे कमजोर प्रक्षुब्ध यांत्रिक मिश्रण हुआ। नतीजतन, थर्मल और यांत्रिक कारकों से प्रक्षुब्ध मिश्रण के प्रभाव के कारण लगातार सकारात्मक और मध्यम गुप्त और संवेदी ऊष्मा प्रवाह (क्रमशः 17.4 और 5.4 डब्ल्यू / एम 2) मान उत्पन्न हुए। मध्याह्न के समय मासिक औसत अल्बेडो बढ़ा था (0.086)। निम्न बोवेन अनुपात (लगभग 0.37) यह भी इंगित करता है कि संवेदी ऊष्मा की तुलना में गुप्त ऊष्मा अधिक निकलती है। जब शुष्क और ठंडी वायु झील के ऊपर से गुजरती है, तो वाष्प का दबाव और वायु का तापमान काफी कम हो जाता है, प्रक्षुब्ध यांत्रिक मिश्रण बढ़ जाता है और ऊर्जा बजट बदल जाता है। परिणामस्वरूप, Ts-Ta, es-ea मान, और संवेदी और गुप्त ऊष्मा प्रवाह सभी बढ़ जाते हैं।

ABSTRACT. In a lake, the heat and energy budgets and evaporation are the most fundamental components of the regional weather and climate and are controlled by the interactions between the lake and the atmosphere. Poyang Lake is the largest freshwater lake in China. The surface area of this shallow lake, located in the central and lower catchment of the Yangtze River, southeastern China, varies across the year based on the precipitation. A steel platform was built in the northeast open-water area of the lake to measure surface energy fluxes and other related atmospheric/hydrologic variables during a cold season from 1 December 2020 to 28 February 2021. The results show the average water surface temperature was 1.25 °C higher than the 2 m height air temperature, though temperature inversions occasionally occurred for short periods. The average wind speed and friction velocity were small, leading to weak turbulent mechanical mixing. Consequently, consistently positive and moderate latent and sensible heat fluxes (17.4 and 5.4 W/m², respectively) values were produced due to the effects of turbulent mixing from thermal and mechanical factors. The monthly average albedo was large at mid-day (0.086). The low Bowen ratio (about 0.37) also indicates that more latent heat is released than sensible heat. When dry and cold air passed over the lake, the pressure of vapor and air temperature decrease significantly, the turbulent mechanical mixing is enhanced and the energy budget changed. As a consequence, the Ts-Ta, e_s-e_a values, and sensible and latent heat fluxes all increase.

Key words – Poyang Lake, Air-water interaction, Turbulent fluxes, Energy budget, Evaporation rate

1. Introduction

Studies show that energy and vapor exchange in the atmosphere mainly originates from interactions between

the atmosphere and land surface. This phenomenon significantly affects the regional and global climate (Webb *et al.*, 1980; Baldocchi *et al.*, 1997; Wang *et al.*, 2010; Gao *et al.*, 2009). Yet, these interactions are very

complex due to surface heterogeneity and seasonal variations (Baldocchi, 1994; Toda *et al.*, 2002; Xue *et al.*, 2004). Simulations of climate are particularly affected by seasonal and momentary variations in the conversion of the surface energy into sensible and latent heat fluxes (Dickinson *et al.*, 1991; Rowntree, 1991). Accordingly, many scholars have focused on seasonal and diurnal deviations in the exchange of influential components such as carbon dioxide and water vapor between the atmosphere and the surface land at different conditions (Hartog *et al.*, 1994; Delire and Gerard, 1995; Betts and Ball, 1995; Campbell *et al.*, 2001; Merquiol *et al.*, 2002; Hu *et al.*, 2006; Liu *et al.*, 2008). The steady-state of the atmosphere is dependent on momentum, heat and moisture surface fluxes (Beljaars and Holtslag, 1991). Atmospheric properties are dependent on surface flux variations (Wang and Eleuterio, 2001), which severely hinders research into the abilities of models to provide accurate simulations of surface variables such as turbulent fluxes (cheng *et al.*, 2014).

Lake systems are one of the fundamental factors that significantly influence ecosystems from a local to the global scale as well as climate by affecting the heat and vapor budgets (Long *et al.*, 2007; Liu *et al.*, 2009), although lakes occupy only 4% of the Earth surface (Downing *et al.*, 2006; Lee *et al.*, 2014; Yang and Lu, 2014). In contrast to oceans, most lakes are widely affected by atmospheric factors because of greater heating or cooling induced by adjacent land surfaces and because of decreased wind speeds (Verburg and Antenucci, 2010). For example, volatile atmospheric properties over lakes can last over longer periods, thereby increasing the loss of latent heat and sensible heat fluxes (Verburg and Antenucci, 2010; Rouse *et al.*, 2003). Large lakes can induce lake-land breezes that influence the regional climate (Cao, *et al.*, 2015; Wang *et al.*, 2017). To understand the hydrological processes and surface fluxes that occur in limnic regions, several comprehensive field experiments and measurements have been carried out around the world over the last decades, and many meaningful results have been obtained (Halldin, *et al.*, 1999, Schertzer, *et al.*, 2003; Hu, *et al.*, 2006; Liu, *et al.*, 2014; Li, *et al.*, 2015, LeMone, *et al.*, 2019). Some studies reveal that the effects of surfaces of inland water bodies on the evaporation and surface energy differ from those of semiarid and vegetated surfaces, and even from those of surfaces of lakes on the plateau (Eaton *et al.*, 2001). Further investigations reveal that albedo of vegetated and water surfaces are 0.08 and 0.06, respectively, indicating that the lake water absorbs a significant proportion of solar radiation (Betts and Ball, 1997; Liu *et al.*, 2005). As a result, the temperature of lake water typically significantly exceeds that of the land surface during winter, whereas the opposite occurs during summer, thereby

introducing a large thermal lag into the climate system of the region.

Furthermore, in lake regions, the Bowen ratios are very low (~0.3 or lower), resulting in the majority of energy released from the water being driven by evaporation to a greater degree than sensible heating of the atmosphere (Liu *et al.*, 2008, 2009). The surface energy balance (SEB) is difficult to close, and energy imbalances always occur (Liu *et al.*, 2008; Li *et al.*, 2016; Grachev *et al.*, 2020).

The performed literature survey reveals that further investigations are required on the lake-air interactions to improve the numerical models in this regard. To this end, it was intended to measure ancillary atmospheric/water variables in a large northeastern open-water area of Poyang Lake during a cold season starting on 1 December 2020. Then observation data were employed to analyze the heat flux, evaporation rate, and surface energy budget. The main objective of the present study was to obtain an improved understanding of how environmental variables influence the heat transfer mechanism and evaporation of the surface of Poyang Lake in a cold season.

The obtained results are expected to improve understanding of the properties of water-air interactions in this lake region and for improving the simulation abilities of the modern climate or weather models.

The structure of the article is as follows. Data and methods; the site and data descriptions, and the methods used to estimate the related variables and variables are introduced in Section 2. Section 3 shows the results of the analyses. Finally, Section 4 provides a discussion and conclusions.

2. Site description, instruments and methods

Poyang Lake is the largest freshwater lake in China, located in the coordinates (28° 24' N - 29° 46' N, 115° 49' E - 116° 46' E) and 2,000 km east of Qinghai-Tibet Plateau. It is a shallow lake with a varying area in the central and lower catchment of the Yangtze River, southeastern China. The lake occupies an average area of ~3,200 km², varying between 500 - 4,200 km². The average depth of this lake is ~8.4 m, but the depth varies significantly with the season. As one of the most important factors, the lake has an important function in regional weather, climate and ecosystems. In November 2020, we built a steel platform in the northeast open-water area of the lake (29° 10' 23" N, 116° 37' 13" E) to measure the surface fluxes, radiation fluxes, water temperature and other meteorological variables, including wind direction

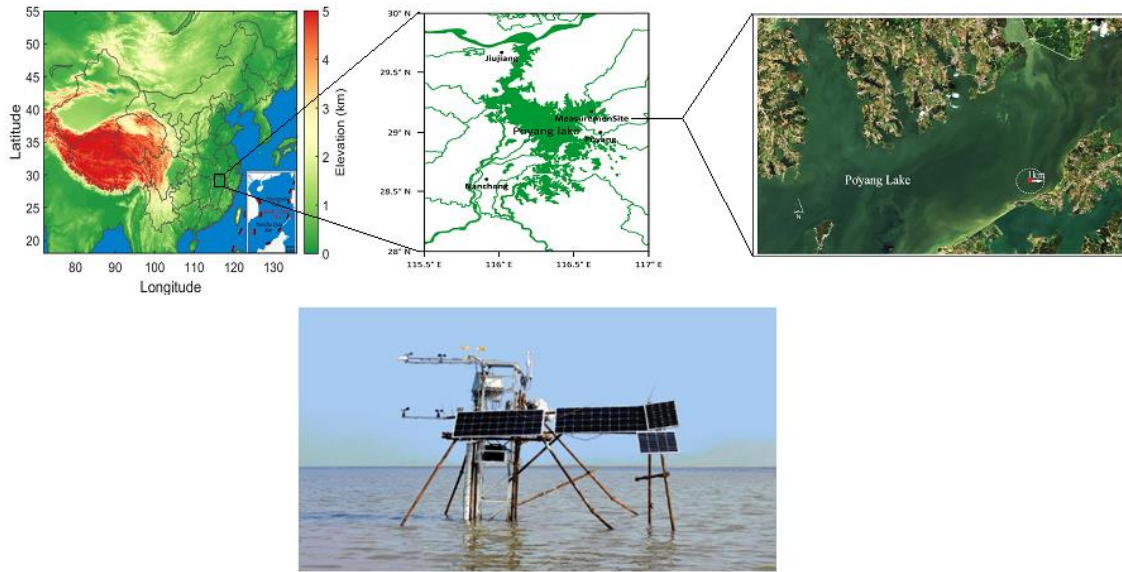


Fig. 1. Satellite image from ESA (European Space Agency) showing the location of the observation platform (29°10'23" N, 116°37' 13" E), denoted by a small pentagram, in the northeast open-water area of Poyang Lake (upper). In addition, a photo of the observation system is provided (below)

and speed and the relative humidity and temperature of the air over the water (Fig. 1). The platform is ~ 3.7 m and 3.2 m above the lakebed and water surface, respectively with fetches ranging from 1.0 km to > 10.0 km. During the observation period, the depth of water around the platform was about 0.5 m. In the present study, a three-dimensional sonic anemometer (100 Hz; UAT-2, IAP, China) and an open-path CO₂/H₂O infrared gas analyzer (10 Hz; LI 7500, LI-COR Inc., China) were arranged at a steel beam in the north eastern section of the platform. Moreover, a data logger (CR6, Campbell, USA) was used to record raw time series data. Two-component shortwave radiometers (MR-60, EKO) were installed on a mounting arm in the southwest section of the platform, and the raw time series data were recorded and stored every minute by a CR3000 data logger. The direction and speed of the wind and relative humidity and temperature of air temperature were measured at two heights (*i.e.*, 2.6 m and 3.7 m above the lakebed) by automatic meteorological stations (JUYING), and the raw time series data were recorded and stored every minute by a GPRS-0408A data logger. The water surface temperature and three layers of water temperatures (0.15 m and 0.35 m below the water surface and 0.1 m in the silt below the lakebed; instruments installed at the end of January) were measured by infrared radiation thermometers and a four-way temperature transmitter (PT100, Heraeus). The raw time series data were recorded every 1 min and were stored in a CR300 data logger.

The original 10-Hz and 100-Hz time-series data were checked for spiking/noise. Data points exceeding 4σ the 30-min average (where σ denotes the standard deviation) were replaced by "NaN". The 3D rotation method [xx] was chosen to rotate the system of coordinates and meet the following conditions: $\overline{w'v'} = 0$, $\overline{w} = 0$, and $\overline{v} = 0$. Fluxes were calculated after a linear trend removal. Latent and sensible heat fluxes (LE and H, respectively), and variations of the vertical velocity (w') moisture content of air (q') and air virtual temperature (T') were calculated every 30 minutes through the average covariance method. Finally, the 30-min flux data failing the quality check were ignored (Vickers and Mahrt, 1997); under these circumstances, the average of the adjacent two data points are used instead of the original data.

In addition to the turbulent fluxes, the meteorological variables (*i.e.*, the temperature and relative humidity of air and wind direction and speed), two-component radiation fluxes and net shortwave radiation, water surface temperatures and water body temperatures were also processed to 30-min averages.

During the measurement period, the rainfall was measured by an infrared rain gauge every 1 min.

Two solar panels and six deep-cycle batteries were utilized as the power source for all instruments. The two

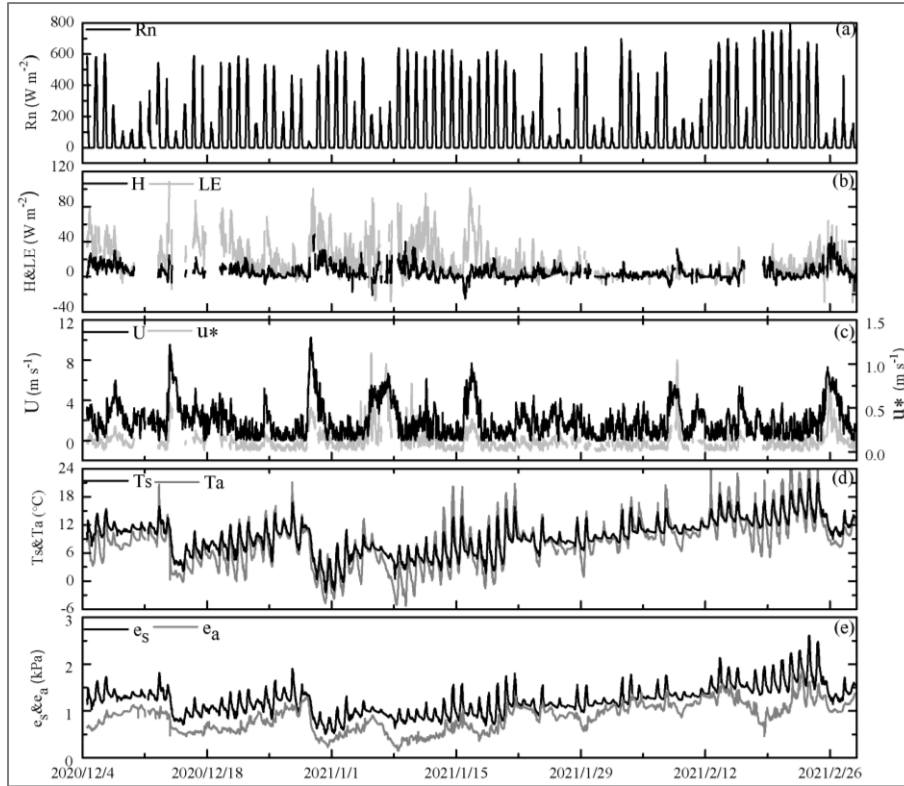


Fig. 2. 30-min time-series of (a) R_n , (b) H and LE heat fluxes, (c) U and u^* , (d) T_s and T_a and (e) e_s and e_a in the cold season

solar panels were installed 1 m east of the platform and 2-2.5 m above the lakebed, below the platform.

The following equations were employed to calculate the related variables:

$$F_{\theta_s} = \overline{w'\theta'} \quad (1)$$

$$F_{q_s} = \overline{w'q'} \quad (2)$$

$$F_{bs} = \frac{g}{\theta_a} F_{\theta_s} + 0.61gF_{q_s} \quad (3)$$

$$L = -\frac{u_*^3}{F_{bs}} = -\frac{u_*^3}{\frac{g}{\theta_n} \overline{w'q'} + 0.61g\overline{w'q'}} \quad (4)$$

$$H = pC_p \overline{w'\theta'} \quad (5)$$

$$LE = pL_v \overline{w'q'} \quad (6)$$

$$H_B = pC_p C U (\theta_s - \theta_a) \quad (7)$$

$$LE_B = pC_E U (e_s - e_a) \quad (8)$$

$$Bo = H / LE \quad (9)$$

$$a = S_o / S_i \quad (10)$$

Where F_{θ_s} and F_{q_s} are the temperature flux and the humidity flux computed through the EC (eddy covariance) method, F_{bs} is the near-surface buoyancy flux, and $\zeta = z/L$ is the atmospheric surface layer (ASL) stability parameter.

3. Results

In southern China, the cold season includes the three months of December, January and February. Analysis of the data measured over the past 50 years at the Poyang meteorological station 20 km south of the observation site showed that the annual average air temperature and precipitation are 17.97 °C and 1,638 mm, respectively. Broadly, the wind speeds and directions varied greatly

throughout the whole year and the air masses had significantly different temperature and humidity properties throughout the whole year due to different synoptic activities in a different season (for example, cold fronts in winter, subtropical highs in summer, tropical cyclones in summer and autumn, troughs and shear lines in the rainy season, *etc.*). The monthly average temperatures (precipitation totals) over the past 50 years were 7.71 °C (51.5 mm), 5.58 °C (78.0 mm) and 7.73 °C (112.4 mm) in December, January and February, respectively. During our observation period, the monthly average air temperatures at the Poyang meteorological station (at our measurement site) were 7.5 °C (6.81 °C), 7.0 °C (6.02 °C) and 12.9 °C (12.22 °C) in December, January and February, respectively. The monthly accumulative precipitation rates at the meteorological Poyang station (at our measurement site) measured from December to February were 20.4 mm (6.8 mm), 8.1 mm (9.8 mm), and 97.6 mm (33.4 mm), respectively. The cold season during which our measurements were made was characterized by drier and warmer conditions compared to the average conditions of cold seasons over the past 50 years. The temperature at our measurement site was lower than that recorded at the Poyang meteorological station, which is in an urbanized area. The precipitation was somewhat evenly distributed. Therefore, under climate change conditions, exchanges of heat and moisture by this open water body in the south with the atmosphere will change through the exertion of diverse atmospheric forcings.

3.1. Intermonthly variations

The net shortwave radiation, R_n , presented obvious diurnal variations, with maximum and minimum values at noon and night, respectively [Fig. 2(a)]. The effects of clouds always induced the daily variations in R_n . For each month, the average R_n was always positive (Table 1), which provided the energy source for this southern open water body during this cold season. From December 2020 to February 2021, the maximum daily average R_n increased from 600 Wm^{-2} in December 2020 to 800 Wm^{-2} in February 2021. Therefore, the monthly average R_n value increased from 87 Wm^{-2} in December 2020 to 112 Wm^{-2} in February 2021 (Table 1).

From December 2020 to February 2021, the wind speed was $\sim 2 m s^{-1}$ on average, resulting in weak turbulent mixing in this region. However, wind speeds varied significantly due to different synoptic weather events. When cold air invaded, wind speeds could be driven to 8-10 ms^{-1} [Fig. 2(c) and Table 1]. Strong cold air processes invaded in December more than in January and February, causing the wind speeds in December to be larger than those in January and February. Consequently, the water waves were higher and more frequent in

TABLE 1

Simple success of rainfall forecast for Jalandhar

Seasons	Post-monsoon (Oct-Jan)	Winter (Feb-Mar)	Rabi (Nov-Apr)
YY (Days)	5	1	7
YN (Days)	4	5	8
NY (Days)	3	2	9
NN (Days)	111	51	157

December than in January or February, causing the albedo, α , to be larger in December (Table 1). The average midday albedo values were 0.104, 0.079 and 0.075 in December, January and February, respectively. The friction velocity, u_* , varied much like U and fluctuated greatly from 0 ms^{-1} to $\sim 1.0 ms^{-1}$. When cold air intruded, u_* increased sharply. On average, u_* was quite small; the monthly average u_* values were 0.12, 0.14 and 0.11 in December, January and February, respectively [Fig. 2(c) and Table 1]. The air temperatures, T_a , in December and January were much lower than those in February, although the temperatures in all months were higher than their average states over the last 50 years. In February, T_a was much higher due to less cold air activities and more sunshine. The water surface temperature similarly varied with time but with more lagging than T_a [Fig. 2(d) and Table 1]. The monthly average T_a (or T_s) was the lowest at 6 °C (7.1 °C) in January and then increased significantly to 12.2 °C (12.8 °C) in February. Accordingly, the difference between T_s and T_a (ΔT) decreased greatly from 2.19 °C in December to 0.62 °C in February (Table 1). The pressure of vapor e_s and e_a exhibited a similar pattern as those of T_s and T_a [Fig. 2(e)], increasing from December to January and then decreasing in February. Especially, the monthly average $T_s(e_s)$ consistently exceeded the monthly average $T_a(e_a)$, although the disparities between T_s and T_a (e_s and e_a) decreased over time (Table 1). The constantly positive differences between T_s and T_a always resulted in an unstable stratification structure over the surface of the water, as demonstrated by the stability of the ASL (ζ) values shown in Table 1 and Fig. 5. And the gradient of the pressure of vapor over the water surface was also always positive, therefore, positive LE and H occurred over the entire season (Table 1). The H (LE) values were 8.2 (26.7), 3.6 (18.6) and 4.3 (7.0) $W m^2$ in December, January and February, respectively. Obviously, LE far exceeded H, with the largest difference in December. There was a clear change in the Bowen ratio (0.31, 0.2, and 0.61 in December, January and February, respectively) (Table 1). These small values of the Bowen ratio showed that the

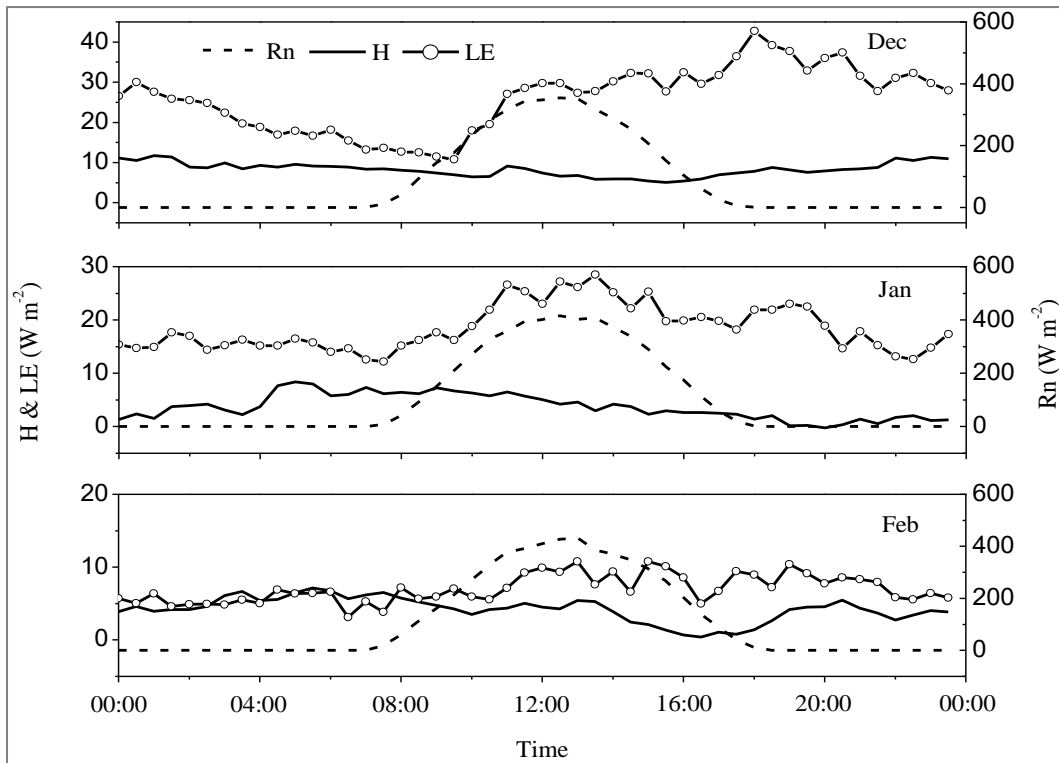


Fig. 3. Average diurnal cycles of Rn, H and LE heat fluxes in different months: (a) December, (b) January and (c) February

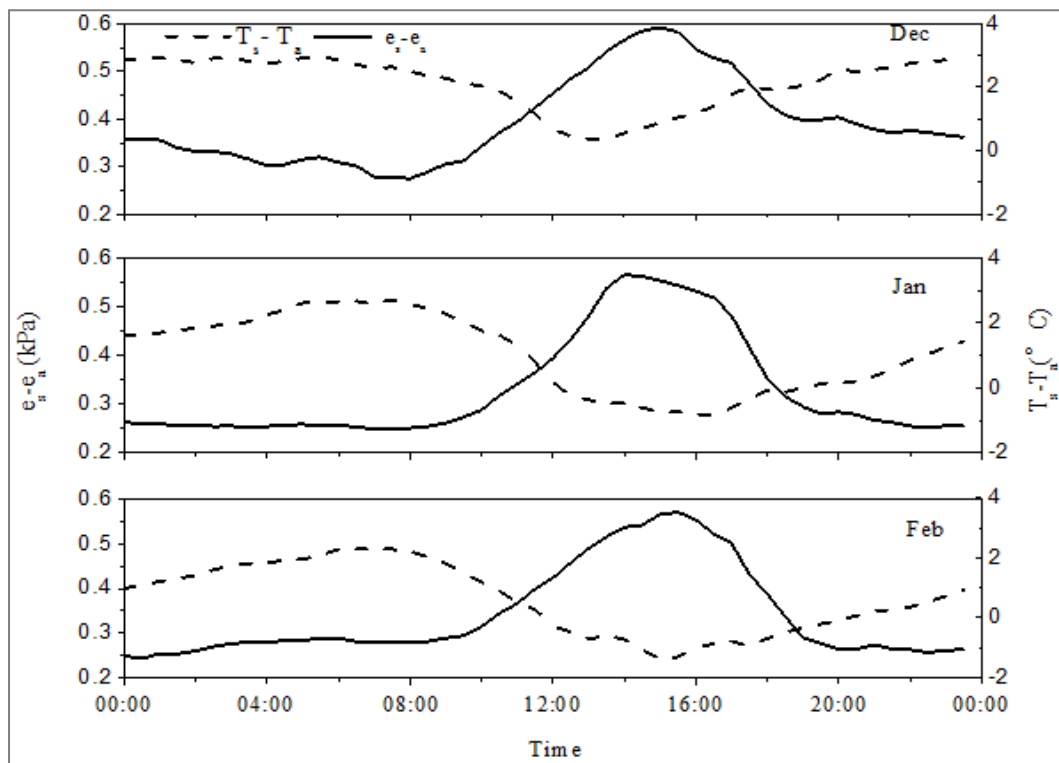


Fig. 4. Average diurnal cycles of differences in temperature between T_s , T_a , e_s and e_a indifferent months: (a) December, (b) January and (c) February

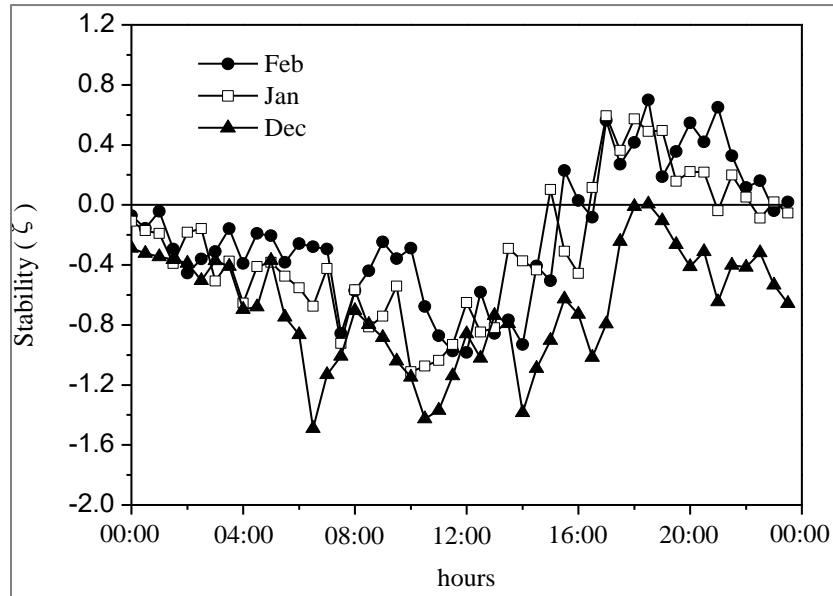


Fig. 5. Average diurnal cycles of ASL stability (ζ) in December, January and February

majority of energy released from water is caused by evaporation rather than sensible heat of the atmosphere.

As shown by the 30-min time-series data, H and LE fluctuated clearly with time and decreased as the months progressed, dissimilarly to the patterns observed for Rn (Fig. 2). Negative H and LE values occasionally appeared, and these values did not always occur at night but were related to weather conditions, such as cold air intrusions or rainfall events. It is noteworthy that either H or LE became quite small from mid-January to late February, which may be because during this period, the temperature was abnormally higher and cold air events were more infrequent than in normal years. As a consequence, ΔT decreased, causing the sensible heat turbulent fluxes to weaken (see sections 3.2 and 3.3 for detailed analyses).

3.2. Diurnal variations

Throughout the entire cold season, the diurnal average Rn exhibited a significant bell-shaped pattern with maximum values around noon and minimum values at night (Fig. 3). LE was always positive and its maximum and minimum values occur in the afternoon and before sunrise, respectively, indicating that consistent evaporation occurs throughout the day. This phenomenon is especially more pronounced during the daytime. This diurnally averaged LE has a close correlation with diurnally averaged $e_s - e_a$ (Fig. 4) in each month. It is found that the maximum and minimum values of $e_s - e_a$ occur in the afternoon and at night, respectively.

TABLE 2

Critical values of error structure for usability analysis of MRWF

Usability	Rainfall (mm)	
	(≤ 10 mm)	(>10mm)
Correct	Diff ≤ 0.2 mm	Diff $\leq 2\%$ of the observed
Usable	$0.2 \text{ mm} < \text{Diff} \leq 2.0$ mm	$0.2 \text{ mm} < \text{Diff} \leq 20\%$ of the observed
Unusable	Diff > 2.0 mm	Diff $> 20\%$ of the observed

However, the diurnal variations in H in each month presented somewhat different patterns. In December, larger H values occurred at night and smaller H values occurred in the daytime. The H values exhibited similar diurnal variations in January and February, with the maximum H values appeared during the early morning (*i.e.*, 05:00-06:00 LT) and minimum ones appeared during the late afternoon (17:00-18:00 LT). These diurnal changes in H were highly related to diurnal fluctuations in $T_s - T_a$. Moreover, Fig. 5 illustrates that the diurnal variations in $T_s - T_a$ affect the ASL stratifications. A comparison between Fig. 5 and Fig. 4 shows that during the studied cold season, the ASL was always unstable except in the late afternoon and the evening before midnight. When $T_s - T_a$ reached its maximum values in the early morning, the ASL became strongly unstable.

TABLE 3

Agromet Advisories prepared and followed along with economic benefit

Date and amount of rainfall forecast	Advisory given and followed 4 days prior	Economic benefit
12 December - 6.0 mm 13 December - 1.0mm	Farmers are advised to skip the irrigation	One irrigation
3 January - 4.0 mm, 4 January - 15.0 mm 5 January - 25.0 mm 6 January - 9.0 mm 7 January - 5.0 mm	Farmers are advised not to irrigate the crop. Also spraying of pesticides/fungicides should be avoided	Spray of fungicide and one irrigation
24 January - 3.0 mm	Farmers are advised to do farm operation (irrigation, spray of pesticides/fungicides) according to the weather forecast	Spray of pesticides/fungicide and one irrigation
13 March - 14.0 mm	Farmers are advised to skip the irrigation	One irrigation

TABLE 4

Seasonal rainfall forecast trends for Jalandhar

Seasons	Ratio score	HSS Score	Bias Score	False Alarm Ratio(FAR)	Probability of Detection	Threat Score
Post-monsoon (Oct-Jan)	94.3	0.56	1.13	0.44	0.63	0.42
Winter (Feb-Mar)	88.1	0.17	2.00	0.83	0.33	0.13
Rabi (Nov-Apr)	90.6	0.40	0.94	0.53	0.44	0.29

TABLE 5

Usability analysis and RMSE of rainfall forecast for Jalandhar

Seasons/Usability (%)	Correct (%)	Usable (%)	Unusable (%)	RMSE (mm)
Post-monsoon (Oct-Jan)	90	3	7	0.45
Winter (Feb-Mar)	85	10	5	0.48
Rabi (Nov-Apr)	86	6	8	0.32

TABLE 6

Yield and yield attributes of wheat during Rabi 2020-21 at Jalandhar

Treatments	Effective tillers/m ²	Ears /Plant	Grains no. /ear	Test weight	Grain yield	Biomass yield
Dates of sowing (DOS)						
15th November	170	12	39	40.1	19.99	39.9
5th December	168	9	21	31.8	19.2	38.4
CD (0.05)	NS	2.2	1.7	1.8	NS	NS
Agromet Advisory Services (AAS)						
Adopted (T1)	169	11	31	33.5	21.1	42.1
Non-adopted (T2)	168	10	29	30	18.1	36.2
CD (0.05)	NS	NS	1.7	1.8	0.8	1.7
Interaction (DOS x AAS)	NS	NS	2.5	2.6	1.2	2.5

TABLE 7

Comparative analysis of cost of cultivation in wheat during Rabi 2020-21 at Jalandhar

Inspects for the crop	15 th November, 2020-21				5 th December, 2020-21			
	AAS farmers		Non-AAS farmers		AAS farmers		Non-AAS farmers	
	Quantity	Cost/acre	Quantity	Cost/acre	Quantity	Cost/acre	Quantity	Cost/acre
Seed	40	1200	40	1200	40	1200	40	1200
Seed treatment	150	50	300	100	150	50	300	100
Fertilizer								
Urea	110	595	110	595	110	595	110	595
DAP	55	1238	55	1238	55	1238	70	1575
Potash			20	392			20	392
Pesticide/Herbicides								
Stomp 30 EC (ml)	1000	500	2000	1000	1000	500	2000	1000
Tilt 25 EC (ml)	200	210	400	420	200	210	400	420
Actara 25 WG (g)	-	-	40	200	-	-	40	200
Gypsum	-	-	100	600	-	-	100	600
Human labour	14	4928	17	5984	14	4928	17	5984
Machine labour	7	2500	7	2500	7	2500	7	2500
Irrigation	3	180	5	300	3	180	5	300
Harvesting	-	3100	-	3100	-	3100	-	3100
Total cost (Sum of all above)	-	14501	-	16437	-	14501	-	16774
Gross return	21.1	37980	19.9	35820	19.2	34560	18.1	30780
Net Return (Total VOP- Total cost)	-	23479	-	19383	-	20059	-	14006
B, °C	-	1, °2.6	-	1, °2.2	-	1, °2.4	-	1, °1.8

As shown in Fig. 2, negative values of H or LE were occasionally observed during the measurement period, which may be because all the available data we dealt with included cloudy and rainy periods; under these conditions, many of the diurnal H and LE signals are removed, and the diurnally averaged H and LE become different from those shown in Fig. 2.

The magnitude of latent or sensible heat flux is related directly to the difference in temperature (pressure of vapor) between the surface of water and the overlying atmosphere, and also depends on turbulent mixing intensity. In numerical models, bulk aerodynamic

algorithms, as shown in equations (7) and (8) in section 2, are broadly applied to estimate the values of H and LE. The relationship between H (LE) and $U\Delta T$ ($U\Delta e$) shown in Figs. 6(a&b) shows that H (LE) increased significantly with $U\Delta T$ ($U\Delta e$), which suggested that these can be represented by equations (7) and (7). On average, H (LE) increased with wind speed U [Figs. 6(c&d)]. However, when the wind speed was small (less than 4.0 ms^{-1}), H (LE) correlated poorly with U, and when U increased to more than 4.0 ms^{-1} , H (LE) increased obviously with U.

In the cold season, cold air masses passed over Poyang Lake frequently (Figs. 7&8). The main wind

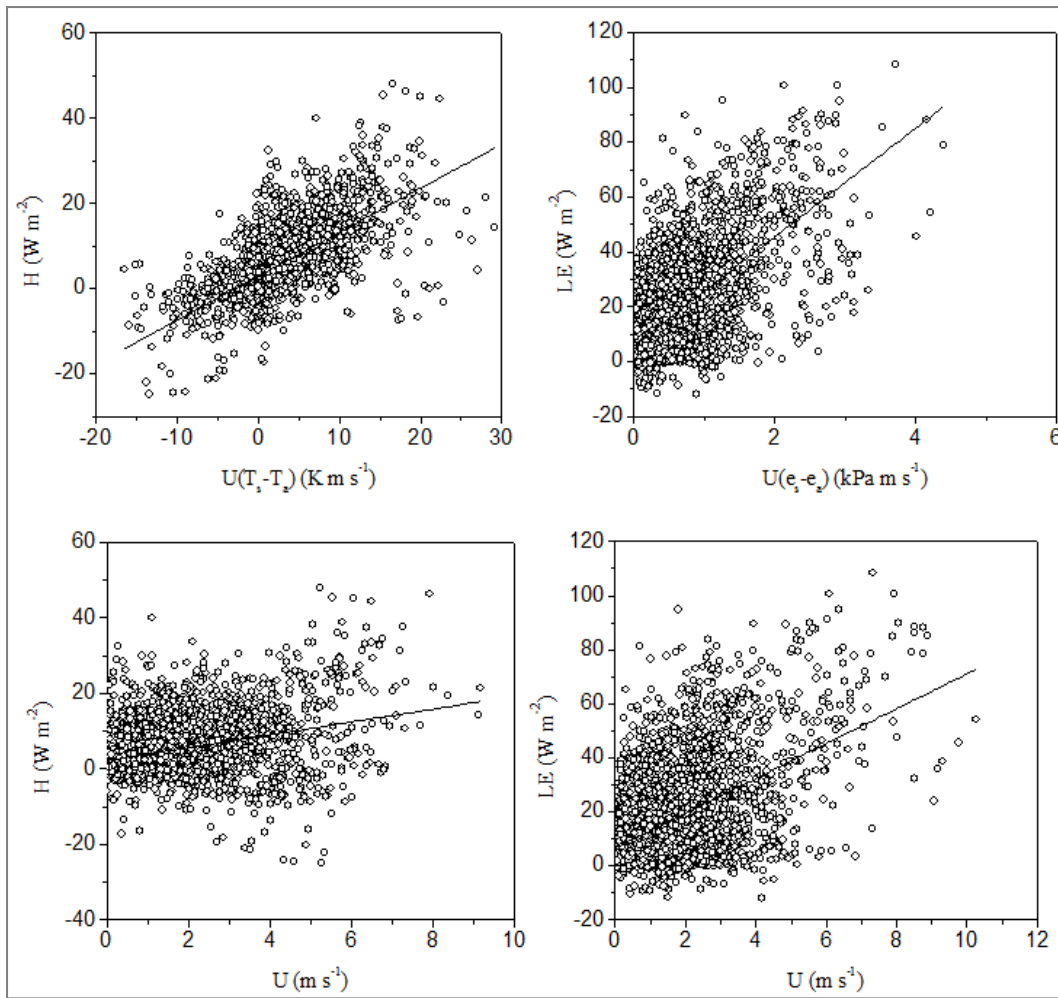


Fig. 6. Relationships between 30-min time-series of (a) H and U(T_s-T_a), (b) LE and U(e_s-e_a), (c) H and U and (d) LE and U

directions shown in the wind rose (Fig. 7) were NNW and NW in this cold season (17% and 13%) and there were about 50% wind came from the second quadrant (between North and West). There were about 80% wind speed below 3 m/s, and only 6% wind speed exceeds 5 m/s.

From 29 December 2020 to 17 January 2021, at least 3 cold air processes passed over the measurement site (Fig. 8). The first process came at our measurement site at about 0700 LT on 29 December 2020, causing an increase of the wind speed from 0.5 to about 10 m s⁻¹ [Fig. 8(a)], a decrease of the air temperature from 11 to -5 °C [Fig. 8(b)] and the atmospheric pressure of vapor from 1.3 to 0.2 kPa [Fig. 8(c)] during the first stage of this process. During this period of cold air influence, the temperature of the water surface, T_s, exceeded that of the overlying air, T_a [Fig. 8(b)], which formed thermally convective stratification. And the pressure of vapor near the water

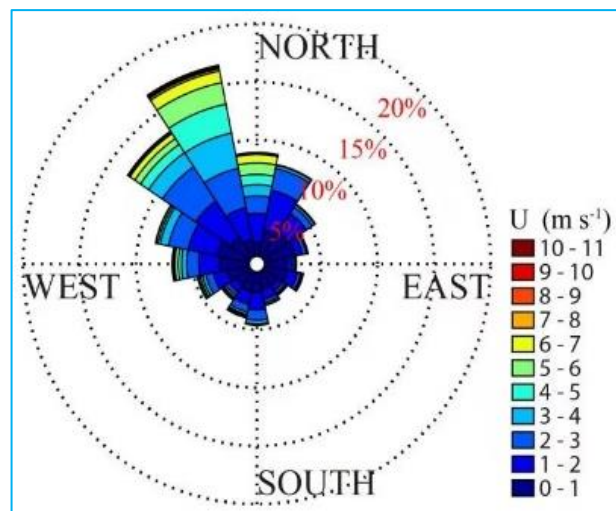


Fig. 7. Wind rose of 16 wind directions in the cold season

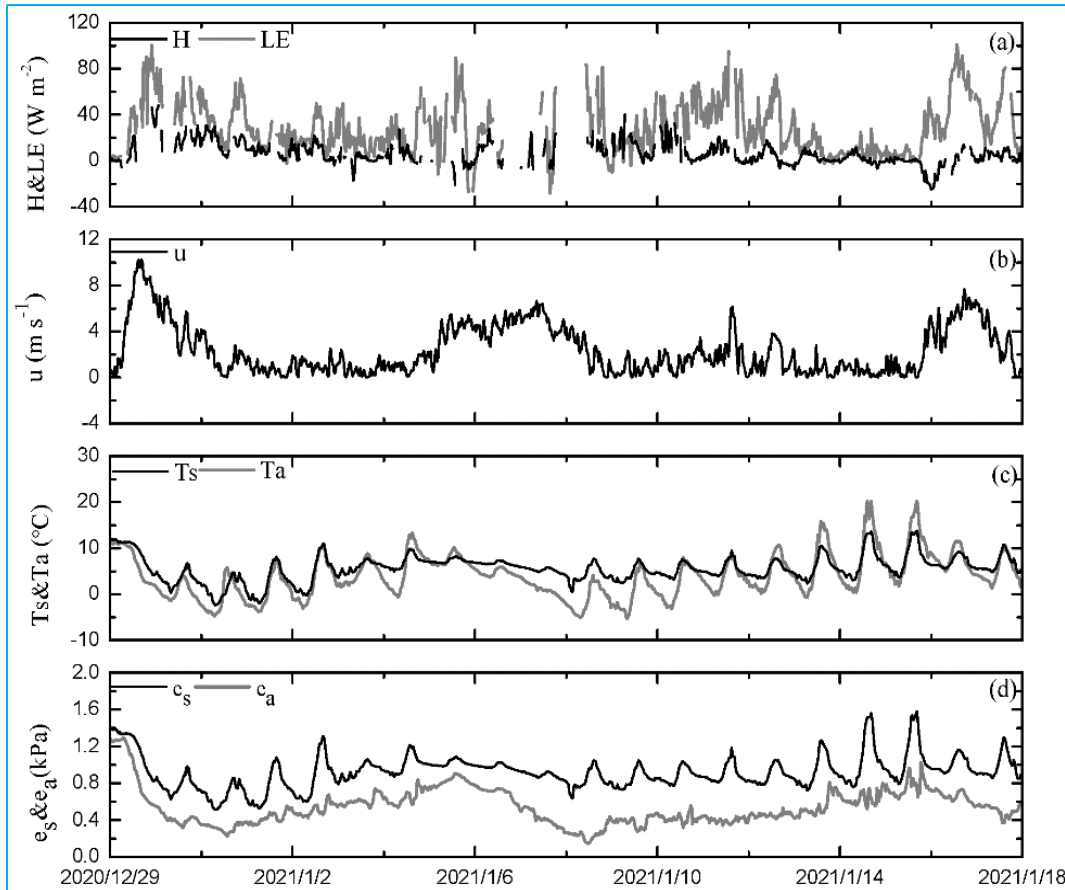


Fig. 8. 30-minute-series of (a) H and LE heat fluxes, (b) U, (c) T_a and T_s and (d) e_s and e_a from 29 December, 2020 to 17 January, 2021

surface, e_s , exceeded that of air, e_a . Additionally, the significant increase in wind speeds mechanically enhanced turbulent mixing. The combined effect of all these factors significantly impacted the turbulent exchanges of H and LE. H increased from ~ -5 to 48 W m^{-2} , and LE increased from ~ 8 to 100 W m^{-2} . And then, H and LE subsequently decreased steadily [Fig. 8(d)]. The second process occurred from 1000 LT on 05 January 2021 to 1000 LT on 08 January 2021, lasting ~ 72 h. During this period, U increased from ~ 2.0 to 6.6 m s^{-1} , the air temperature decreased from 10.0 to $-5 \text{ }^\circ\text{C}$, and the pressure of vapor dropped from 1.1 to 0.15 kPa (Fig. 8). Temperature of the water surface, T_s , far exceeded that of the overlying air, T_a [Fig. 8(b)] and the pressure of vapor of the air e_a was much lower than the pressure of vapor near the water surface e_s . H increased from ~ -5 to 28 W m^{-2} , and LE increased from ~ 32 to 89 W m^{-2} . The third process occurred from ~ 1900 LT on 15 January 2021 to 1100 LT on 17 January 2021 and lasted for ~ 40 h. During this period, U increased from ~ 1.0 to 8 m s^{-1} , the temperature of air decreased from 12.0 to $1 \text{ }^\circ\text{C}$, and the

pressure of vapor declined from 1.0 to 0.36 kPa (Fig. 8). The temperature of the water surface T_s far exceeded that of the overlying air T_a [Fig. 8(b)] and the pressure of vapor near the water surface, e_s , far exceeded that of air, e_a . H increased from ~ -24.0 to 14 W m^{-2} , and LE increased from ~ 20.0 to 100 W m^{-2} . The results of the 3 processes indicated that when cold and dry air passed over the lake, the air temperature and pressure of vapor decreased significantly; as a consequence, $T_s - T_a$ and $e_s - e_a$ increased, as did H and LE.

4. Conclusions

In this paper, the cold season measurements of components of the surface energy budget, microclimate variables, and evaporation rates 4 December 2020 to 28 February 2021 over Poyang Lake were used to explore the interactions between the air and the lake. The key findings of this study are summarized as follows. In this cold season, the monthly average water surface temperature T_s ($9.63 \text{ }^\circ\text{C}$) was always higher than T_a ($8.36 \text{ }^\circ\text{C}$), suggesting

that unstable ASL plays a major role in this cold season. The larger monthly average pressure of vapor difference ratio (about 29%) indicates the possibility of strong vapor evaporation. The monthly average wind speed (1.94 ms^{-1}) and friction velocity u_* (0.12 ms^{-1}) were small and mechanically suppressed mixing. Consistently moderate and positive H and LE values were consequently generated due to the combined effects of the mechanically and thermally generated turbulent mixing. The monthly average shortwave radiation, R_n , was 101.6 W m^{-2} , ranging from 87.4 to 112 W m^{-2} , the average H value was 5.4 W m^{-2} , ranging from 8.2 to 3.6 W m^{-2} , and the average LE value was 17.4 W m^{-2} , ranging from 7.0 to 26.7 W m^{-2} . The monthly average albedo at mid-day was large (0.086). The low Bowen ratio (about 0.37) also indicates that the latent heat is released more than the sensible heat.

5. Discussion

As the largest freshwater lake in China, Poyang Lake is a shallow lake with a varying area. During our measurements, the depth of the lake around the measurement platform was only $\sim 0.5 \text{ m}$, although the fetch reached 1-10 km. This condition may result in different heat and vapor exchanges occurring between the air and water from those that occur over other open waters. The results showed that either the wind speed U or the pressure of vapor over the lake was smaller in magnitude than that observed by Liu *et al.* (2012) over a lake in Mississippi, although the two lakes are located at almost the same latitude ($\sim 30^\circ \text{ N}$). As a consequence, the latent and sensible heat fluxes over Poyang Lake were quite small. The diurnal variations in the latent and sensible heat fluxes corresponded rather better differences in temperature and pressure of vapor between the water surface and overlying air than did the solar radiation. The ASL over the lake was always unstable, especially at night. However, in the afternoon, as time went on, the ASL became weakly unstable and even became transitorily stable before nightfall. Therefore, the maximum sensible heat flux H always occurred at night, and the minimum H appeared in the afternoon. The albedo of this shallow lake surface was ~ 0.086 , larger than the values observed over other lakes (Liu *et al.*, 2012). The average Bowen ratio during the studied cold season was 0.37 for Poyang Lake, which was significantly lower than that measured for the *Myricaria squamosa* Desv. shrubs in the Qinghai Lake watershed (average value was 1.67 from May 2010 to March 2013) (Zhang *et al.*, 2014).

In the cold season, cold air masses passed over Poyang Lake frequently. When these dry and cold air masses passed above the lake, the air temperature and pressure of vapor decreased significantly. As a

consequence, $T_s - T_a$ (1.27°C) and $e_s - e_a$ (>0) increased, as did H (5.4 W m^{-2}) and LE (17.4 W m^{-2}).

The results of this study can provide a better knowledge of the fluxes of surface water vapor and the surface energy budget of Poyang Lake and its role in moderating the local climate. Consistent ASL instability at night and in the early morning would increase evaporation from the lake thermally, and a smaller average wind speed would mechanically lead to weak turbulent mixing. At times in January and February, H was slightly negative due to the existence of inversions ($T_a > T_s$) in the afternoon. Therefore, the effects of the interactions among the air temperatures, surface water temperatures, and wind speeds in driving the surface energy budget and evaporation need further deep investigations in the future, especially via comparisons with model results.

Acknowledgments

This study was jointly supported by the National Natural Science Foundation of China under grants 41765001, 41265003 and 40633017.

Disclaimer : The content and views expressed in this study are the views of the authors and do not necessarily reflect the views of the organizations they belong to.

References

- Baldocchi, D. D., Vogel, C. A. and Hall, B., 1997, "Seasonal variation of energy and water vapor exchange rates above and below a boreal jackpine forest canopy", *J. Geophys. Res.*, **102**, D24, 28, 939-28,951, doi : 10.1029/96JD03325.
- Baldocchi, D. D., 1994, "A comparative study of mass and energy exchange over a closed C3 (wheat) and an open C4 (corn) canopy, I. The partitioning of available energy into latent and sensible heat exchange", *Agric. For. Meteorol.*, **67**, 191-220.
- Beljaars, A. C. M., and Holtslag, A. A. M., 1991, "Flux parameterization over land surfaces for atmospheric models", *J. Appl. Meteorol.*, **30**, 327-341.
- Betts, A. K. and Ball, J. H., 1995, "The FIFE surface diurnal cycle climate", *J. Geophys. Res.*, **100**, D12, 679-693.
- Betts, A. K., and Ball, J. H., 1997, "Albedo over the boreal forest", *J. Geophys. Res.*, **102**, 28, 901- 28, 909. doi : 10.1029/96JD03876.
- Campbell, C. S., Heilman, J. L., McInnes, K. J., Wilson, L. T., Medlay, J. C., Wu, G. and Cobos, D. R., 2001, "Diel and seasonal variation in CO_2 flux of irrigated rice", *Agr. Forest Meteorol.*, **1**, 108, 15-27.
- Cao, J. H., Liu, X. M., Li, G. P. and Zou, H. B., 2015, "Analysis of the phenomenon of lake land breeze in Poyang Lake area (in Chinese)", *Plateau Meteorology*, **34**, 2, 426-436.
- Cheng, X. L., Z. Peng, F. Hu, Zeng, QingCun, Luo, WeiDong, Zhao, YiJun and Hong, ZhongXiang 2014, "Measurement errors and correction of the UAT-2 ultrasonic anemometer", *Sci. China Tech. Sci.*, **58**, "677-686. doi : 10.1007/s11431-014-5728-5.

- Delire, C. and Gerard, J. G., 1995, "A numerical study of the influence of the diurnal cycle on the surface energy and water budgets", *J. Geophys. Res.*, **100**, D3, 5071-5084.
- Dickinson, R. E., A. Henderson-Sellers, C. Rosenzweig, sellers, P., 1991, "Evapotranspiration models with canopy resistance for use in climate models, "A review, *Agric. For. Meteorol.*, **54**, 373-388. doi : 10.1016/0168-1923(91)90014-H.
- Downing, John, Prairie, Yves, Cole, Jonathan, Duarte, Carlos, Tranvik, Lars, Striegl, Robert, McDowell, William, Kortelainen, P., Caraco, N. F., Melack, J. M. and Middelburg, Jack., 2006, "The Global Abundance and Size Distribution of Lakes, Ponds, and Impoundments. *Limnology and Oceanography*, **51**. 2388 - 2397. doi : 10.4319/lo.2006.51.5.2388.
- Eaton, A. K., W. R. Rouse, P. M. Lafleur, Marsh, P. and Blanken, P. D., 2001, "Surface energy balance of the western and central Canadian sub-Arctic. "Variations in the energy balance among five major terrain types", *J. Clim.*, **14**, 3692-3703, doi : 10.1175/1520-0442(2001).
- Gao, Zhiqiu, Lenschow, Donald, He, Zhijun, M, Zhou, Wang, Lisi, Wang, Yajun, J, He, J, Shi., 2009, "Seasonal and diurnal variations in moisture, heat and CO₂ fluxes over a typical steppe prairie in Inner Mongolia", *China. Hydrology and Earth System Sciences Discussions*, **6**. doi : 10.5194/hessd-6-1939-2009.
- Grachev, A. A., C. W. Fairall, B. W. Blomquist, Fernando, Harindra, Leo, Laura, Otárola-Bustos, Sebastián, Wilczak, James, McCaffrey and Katherine, 2020, "On the surface energy balance closure at different temporal scales", *Agric. For Meteorol.*, **281**, 107823.
- Haldin, S., S. E. Gryning, L. Gottschal, A. Jochum, L. C. Lundin and A. A. Van de Griend, 1999, "Energy, water and carbon exchange in a boreal forest landscape-NOPEX experiences", *Agric. For Meteorol.*, **98**, 1, 5-29.
- Hartog, G., Neumann, H. H., King, K. M. and Chipanshi, A. C., 1994, "Energy budget measurements using eddy correlation and Bowen ratio techniques at the Kinosheo Lake tower site during the Northern Wetlands Study", *J. Geophys. Res.*, **99**, D1, 1539-1549.
- Hu, F., Z. X. Hong, J. Y. Chen and X. M. Liu, 2006, "The field experiment of atmospheric boundary layer over heterogeneous surface in Baiyangdian area-introduction and preliminary data analysis (in Chinese)", *Chinese Journal of Atmospheric Sciences*, **30**, 5, 883-893.
- Lee, Xuhui, Liu, Shoudong, Xiao, Wei, Wang, Wei, Gao, Zhiqiu, Cao, Chang, Hu, Cheng, Hu, Zhenghua, Shen, Shuanghe, Wang, Yongwei, Wen, Xuefa, Xiao, Qitao, Xu, Jiaping, Yang, Jinbiao and Zhang, Mi., 2014, "The Taihu Eddy Flux Network: An Observational Program on Energy, Water, and Greenhouse Gas Fluxes of a Large Freshwater Lake", *Bulletin of the American Meteorological Society*. **95**.
- LeMone, Margaret, Angevine, Wayne, Bretherton, Christopher, Dudhia, Jimmy, Fedorovich, Evgeni, Katsaros, Kristina, Lenschow, Donald, Mahrt, Larry, Patton, Edward, Sun, Jielun, Tjernström, Michael and Weil, Jeffrey, 2019, "100 Years Of Progress In Boundary-Layer Meteorology. Meteorological Monographs", **59**. 10.1175/AMSMONOGRAPHS-D-18-0013.1.
- Li, Xiao-Yan, Ma, Yujun, Huang, Y., Hu, Xia, Wu, Xiuchen, Wang, Pei, Li, Guang-Yong, Zhang, Siyi, Wu, Huawu, Jiang, Zhi-Yun, Cui, Buli and Liu, Lei., 2016, "Evaporation and surface energy budget over the largest high-altitude saline lake on the Qinghai-Tibet Plateau: WATER AND ENERGY FLUX OVER QINGHAI LAKE", *Journal of Geophysical Research: Atmospheres*. **121**. 10.1002/2016JD025027.
- Li, Z. G., S. H. Lyu, Y. H. Ao, Wen, L., Zhao, L. and Wang, S., 2015, "Long-term energy flux and radiation balance observations over Lake Ngoring, Tibetan Plateau", *Atmos. Res.*, **155**, 13-25.
- Liu, H. P., J. T. Randerson, J. Lindfors, and F. S. Chapin, 2005, "Changes in the surface energy budget after fire in boreal ecosystems of interior Alaska, "An annual perspective", *J. Geophys. Res.*, **110**, D13101. doi : 10.1029/2004JD005158.
- Liu, Heping, Zhang, Yu, Liu, Shuhua, Jiang, Haimei, Sheng, Li and Williams, Quinton, 2009, "Eddy covariance measurements of surface energy budget and evaporation in a cool season over southern open water in Mississippi", *Journal of Geophysical Research*. **114**. 10.1029/2008JD010891.
- Liu, H. Z., Feng, J. W., Sun, J. H., Lei, Wang and AnLun, Xu 2014, "Eddy covariance measurements of water vapor and CO₂ fluxes above the Erhai Lake", *Scientia Sinica (Terrae)*, **44**, 11, 2527-2539.
- Liu, X. M., F. Hu, J. H. Jiang and C. M. Zhen, 2008, "Energy budget over the water-land heterogeneous surface in Baiyangdian region (in Chinese)", *Chinese Journal of Atmospheric Sciences*, **32**, 6, 1411-1418.
- Long, Z., W. Perrie, J. Gyakum, D. Caya and R. Laprise, 2007, "Northern lake impacts on local seasonal climate", *J. Hydrometeorol.*, **8**, 881-896. doi : 10.1175/JHM591.1
- Merquiol, Emmanuelle, Pnueli, L, Cohen, M, Simovitch, Michal, Rachmilevitch, Shimon, Goloubinoff, Pierre, Kaplan, Aaron and MITTLER, R., 2002, "Seasonal and diurnal variations in gene expression in the desert legume *Retama raetam*", *Plant, Cell and Environment*. **25**. 1627-1638.
- Rouse, Wayne, Oswald, Claire, Binyamin, Jacqueline, Blanken, Peter, Schertzer, William, Spence, Christa, 2003, "Interannual and Seasonal Variability of the Surface Energy Balance and Temperature of Central Great Slave Lake" *Journal of Hydrometeorology – J. hydrometeorol.* **4**.
- Rowntree, P. R., 1991, "Atmospheric parameterization schemes for evaporation over land", "Basic concepts and climate modeling aspects, in *Land Surface Evaporation, Measurement, and Parameterization*, edited by T. J. Schmugge and J. C. André, 5-29, Springer, New York.
- Schertzer, William, Rouse, Wayne, Blanken, Peter, Walker, Anne, 2003, "Over-Lake Meteorology and Estimated Bulk Heat Exchange of Great Slave Lake in 1998 and 1999", *Journal of Hydrometeorology*. **4**. 649-659.
- Toda, M., K. Nishida, N. Ohte, Makoto, TANI, Katumi MUSIAKE, 2002, "Observations of energy fluxes and evapotranspiration over terrestrial complex land covers in the tropical monsoon environment", *J. Meteorol. Soc. Jpn.*, **80**, 465-484. doi : 10.2151/jmsj.80.465.
- Verburg, P. and Antenucci, J. P., 2010, "Persistent unstable atmospheric boundary layer enhances sensible and latent heat loss in a tropical great lake", *Lake Tanganyika, J. Geophys. Res.*, **115**, D11109. doi : 10.1029/2009JD012839.
- Vickers, D. and Mahrt, L., 1997, "Quality control and flux sampling problems for tower and aircraft data", *J. Atmos. and Ocean Tech.*, **14**, 512-526.
- Wang, Guoyin, Huang, Jianping, Guo, Weidong, Zuo, Jinqing, Wang, Jiemin, Jianrong, Bi, Huang, Zhongwei, Shi, Jinsen, 2010 "Observation analysis of land-atmosphere interactions over the Loess Plateau of northwest China", *Journal of Geophysical Research*. **115**. 10.1029/2009JD013372.

- Wang, Q. and Eleuterio, D. P., 2001, "A comparison of bulk aerodynamic methods for calculating air-sea fluxes, paper presented at Ninth Conference on Mesoscale Processes", *Am. Meteorol. Soc.*, Fort Lauderdale, Fla.
- Wang, Yongwei, Gao, Yaqi, Qin, Hairun, Huang, Jianping, Liu, Cheng, Hu, Cheng, Wang, Wei, Liu, Shoudong and Lee, Xuhui, 2017, "Spatiotemporal Characteristics of Lake Breezes over Lake Taihu, China" *J. of Applied Meteorology and Climatology*. **56**.
- Webb, E. K., G. I. Pearman, and R. Leuning, 1980, "Correction of flux measurements for density effects due to heat and water vapour transfer", *Q. J. R. Meteorol. Soc.*, **106**, 85-100.
- Xue, Y. K., H. M. Juang, W. P. Li, Prince. S., R. DeFries, Y. Jiao and R. Vasic 2004, "Role of land surface processes in monsoon development", "East Asia and West Africa", *J. Geophys. Res.*, **109**, D03105. doi : 10.1029/2003JD003556.
- Yang, X. K. and Lu, X. X., 2014, "Drastic change in China's lakes and reservoirs over the past decades", *Sci. Rep.*, **4**, 6041, doi : 10.1038/srep.
- Zhang, S. Y., X. Y. Li, Y. J. Ma, 2014, "Interannual and seasonal variability in evapotranspiration and energy partitioning over the alpine riparian shrub *Myricaria squamosa* Desv. On Qinghai-Tibet Plateau", *Cold Reg. Sci. Technol.*, **102**, 8-20.

